MiR-601-induced BMSCs senescence accelerates steroid-induced osteonecrosis of the femoral head progression by targeting SIRT1

Boyu Tang
The First Affiliated Hospital of Chongqing Medical University
Yu Chen
The First Affiliated Hospital of Chongqing Medical University
Pei Zhao
The First Affiliated Hospital of Chongqing Medical University
Wenlong Yan
The First Affiliated Hospital of Chongqing Medical University
Xiao Huang
The First Affiliated Hospital of Chongqing Medical University
Weiqian Jiang
The First Affiliated Hospital of Chongqing Medical University
Mingjie Sun
The First Affiliated Hospital of Chongqing Medical University
Hongrui Zhang
The First Affiliated Hospital of Chongqing Medical University
Dulei Xiang
The First Affiliated Hospital of Chongqing Medical University
Tingmei Chen
Chongqing Medical University
Chengjie Lian
The First Affiliated Hospital of Chongqing Medical University
jian zhang (zhangjian@hospital.cqmu.edu.cn)
The First Affiliated Hospital of Chongqing Medical University https://orcid.org/0000-0003-2908-1935

Research Article

Keywords: steroid-induced osteonecrosis of the femoral head, bone marrow mesenchymal stem cells, cell senescence, miR-601, SIRT1

Posted Date: April 18th, 2023

DOI: https://doi.org/10.21203/rs.3.rs-2798512/v1

Version of Record: A version of this preprint was published at Cellular and Molecular Life Sciences on August 19th, 2023. See the published version at https://doi.org/10.1007/s00018-023-04903-8.

Abstract

Background: The imbalance between osteogenic and adipogenic differentiation of bone marrow mesenchymal stem cells (BMSCs) is not only the primary pathological feature but also a major contributor to the pathogenesis of steroid-induced osteonecrosis of the femoral head (SONFH). Cellular senescence is one of the main causes of imbalanced BMSCs differentiation. The purpose of this study was to reveal whether cellular senescence could participate in the progression of SONFH and the related mechanisms.

Methods: The rat SONFH model was constructed, and rat BMSCs were extracted. Aging-related indicators were detected by SA-β-Gal staining, qRT-PCR and Western Blot experiments. Using H_2O_2 to construct a senescent cell model, and overexpressing and knocking down miR-601 and SIRT1 in hBMSCs, the effect on BMSCs differentiation was explored by qRT-PCR, Western Blot experiment, oil red O staining, alizarin red staining, and luciferase reporter gene experiment. A rat SONFH model was established to test the effects of miR-601 and metformin in vivo.

Results:The current study showed that glucocorticoids (GCs)-induced BMSCs senescence, which caused imbalanced osteogenesis and adipogenesis of BMSCs, was responsible for the SONFH progression. Further, elevated miR-601 caused by GCs was demonstrated to contribute to BMSC senescence through targeting SIRT1. In addition, the anti-aging drug metformin was shown to be able to alleviate GCs-induced BMSCs senescence and SONFH progression.

Conclusions: Considering the role of BMSCs aging in the progression of SONFH, this provides a new idea for the prevention and treatment of SONFH.

Background

Steroid-induced osteonecrosis of the femoral head (SONFH), which is the most common type of non-traumatic osteonecrosis of the femoral head, is caused by long-term or high-dose GCs use [1]. SONFH can lead to the collapse of the femoral head, followed by the destruction of the hip joint. At the late stage, almost all SONFH patients require total hip arthroplasty. Furthermore, due to the limited service life of the hip prosthesis, quite a number of young patients require repeat arthroplasty [2, 3]. These concerns have led to an increasing demand for hip-sparing techniques. However, the effectiveness of these techniques is still questionable. The effectiveness of core decompression in advanced patients is only 28.6%, while osteotomy requires long-term bed rest, resulting in a series of postoperative complications [2, 3]. Thus, there is an urgent need for effective therapeutic treatment that could block or even reverse the progression of SONFH.

Bone marrow mesenchymal stem cells (BMSCs) with pluripotent differentiation ability play a key role in SONFH, and the imbalance between osteogenic and adipogenic differentiation of BMSCs is considered to be not only the core pathological feature but also an important pathogenesis of SONFH [4, 5]. Under physiological conditions, the adipogenesis and osteogenesis of BMSCs are in a dynamic balance.

However, with the treatment of high-dose GCs, the adipogenic differentiation of BMSCs was enhanced, and the osteogenic differentiation was weakened. A series of pathophysiological changes were caused by disturbed BMSCs differentiation, which eventually led to SONFH [6].

Cellular senescence, a state of permanent cell cycle arrest induced by different destructive stimuli [7], plays a crucial role in the progression of various diseases. In addition, cellular senescence is one of the main factors leading to an imbalance in BMSCs differentiation [8]. Cellular senescence may also occur in young cells; the main hallmarks of cellular senescence are the activation of the chronic DNA damage response, the engagement of various cyclin-dependent kinase inhibitors, enhanced secretion of proinflammatory and tissue-remodeling factors, the induction of antiapoptotic genes, altered metabolic rates, and endoplasmic reticulum stress [9]. In addition, aging has been reported to activate adipogenic differentiation and inhibit osteogenic differentiation of BMSCs by modulating oxidative damage, expression of osteogenesis and adipogenesis-related genes, and cell cycle arrest [8, 10, 11]. Considering the key role of BMSCs differentiation in SONFH, we wondered whether senescence could affect SONFH progression by breaking the balance of BMSCs differentiation and whether anti-senescence therapy could prevent SONFH.

Sirtuin1 (SIRT1) is a NAD^+-dependent deacetylase, and it is a well-known anti-aging molecule that participates in multiple aging-related processes, such as the DNA damage response, the regulation of cyclin-dependent kinase inhibitors, and so on [12]. Aging is associated with the down-regulation of SIRT1. SIRT1 protein, but not mRNA, decreased significantly in senescent mouse embryonic fibroblasts and with serial cell passage in both human and murine cells [13, 14]. On the other hand, SIRT1 regulates the aging process and disease progression, and mice deficient in SIRT1 are smaller and age faster than their wild-type littermates [15]. Furthermore, activation of SIRT1 can determine the differentiation fate of BMSCs, manifested by enhanced osteogenic differentiation and suppressed adipogenic differentiation [11]. However, the role of SIRT1 in the process of SONFH needs further study.

Current research focused on the role of BMSCs senescence in the progression of SONFH, and the miR-601/SIRT1 axis was shown to mediate GCs-induced BMSCs senescence and SONFH progression. Moreover, the therapeutic effect of the anti-aging drug metformin on SONFH was illustrated.

Materials And Methods

1. Animals

Male Sprague-Dawley rats (7 weeks old, weighing 160-220 g) were purchased from the Animal Laboratory in Chongqing Medical University and had free access to food and fresh water at room temperature. Five rats per group were used to ensure adequate power, and rats were randomly allocated into four groups. (1) SONFH group: rats in this group were initially injected with lipopolysaccharide (20 μg/kg; Solarbio, Beijing, China) for 2 days, and then Methylprednisolone (MPS) (60 mg/kg; Pfizer Inc, New York, USA) was injected three times each week in a 24-hour interval for four weeks. (2) SONFH +

antagomir (SONFH + AT) group: rats in this group received the same procedure as the SONFH group to establish the SONFH model. Additionally, on the 7th day, rats were anesthetized with 3% pentobarbital sodium (30 mg/kg), and miR-601 antagomir (5 nmol; GenePharma, Shanghai, China) (AT) was injected into the bone marrow cavity of each femur through the femoral intercondylar fossa according to the manufacturer's instruction. (3) Normal control (Control) group: rats were subjected to normal saline injection and sham operation. (4) SONFH + Metformin (SONFH+Met) group: rats in this group received the same procedure as the SONFH group to establish the SONFH model. Metformin (Solarbio, Beijing, China) was dissolved in drinking water (200 mg/kg) 7 times a week starting on the 7th day, the metformin dosage was converted from the human equivalent dose to the rat dose based on body surface area. The water consumption and body weight of the rats were measured once a week, and the concentration of metformin in the drinking water was adjusted weekly according to changes in water consumption and rat body weight. The rats in all groups were sacrificed at 6 weeks, and the bilateral femoral heads were isolated for subsequent experiments.

2. Source of human femoral heads

Human femoral heads were obtained from patients who underwent total hip arthroplasty (THA) at the First Affiliated Hospital of Chongqing Medical University between 2020 and 2022. (1) SONFH group: SONFH samples were obtained from necrotic areas of the femoral heads of 10 SONFH patients. These patients were classified as grades 3 or 4 according to the Ficat classification system. (2) Femoral neck fracture (FNF) group: FNF samples were obtained from healthy femoral heads of 10 FNF patients. The clinical characteristics of the patients are listed in Supplementary Table 1. All the samples were rapidly stored in liquid nitrogen until they were put to use.

3. Micro-CT

The rat femoral heads were scanned using micro-CT to assess bone mass, density, and trabecular microarchitecture. The femurs were dissected, cleaned, and fixed in 4% paraformaldehyde for 2 days, then scanned using micro-CT with a high-resolution system to evaluate bone repair. The samples were scanned continuously at a resolution of 9 μm per voxel. The 2D images were transferred to CT. A software and the trabecular parameters of the subchondral bone of the femoral head were quantified, including bone volume per tissue volume (BV/TV), trabecular thickness (Tb.Th), trabecular number (Tb.N), and trabecular separation (Tb. Sp).

4. Cell culture and treatments

The human primary BMSCs (hBMSCs) were purchased from Zhong Qiao Xin Zhou Biotechnology (Shanghai, China). hBMSCs were cultured in MSC culture medium (Sciencell, USA) containing 10% fetal calf serum (Gibco, USA) and 1% double-antibody (Biosharp, Guangzhou, China).

For adipogenic differentiation, hBMSCs were induced for 1 week in adipogenic induction medium A consisting of high-glucose DMEM (Gibco, USA) with 10 μg/ml insulin (Beyotime, Shanghai, China), 0.5

mM IBMX (Sigma-Aldrich, Germany), 1 μM dexamethasone (Sigma-Aldrich, Germany), and 200 μM indometacin (Solarbio, Beijing, China). Then, use adipogenic maintenance medium B to maintain adipogenic differentiation of BMSCs for 2 weeks. Adipogenic maintenance medium B consisting of high-glucose DMEM with 10 μg/ml insulin. The medium was changed every 2 or 3 days.

For osteogenic differentiation, hBMSCs were cultured in osteogenic induction medium consisting of high-glucose DMEM (Gibco, USA) with 10^{-2} M β-sodium glycerophosphate (Solarbio, Beijing, China), 50 μg/mL L-ascorbic acid (Solarbio, Beijing, China), and 10^{-7} M dexamethasone (Sigma-Aldrich, Germany). The medium was changed every 2 or 3 days.

For induction of hBMSCs senescence, hBMSCs were cultured in induction medium consisting of 5 mL of complete medium [α-MEM (Sigma-Aldrich, Germany), 10% fetal bovine serum, 1% double- antibody]. The control group was added with 1 μL PBS; the modeling group was added with 1 μL H_2O_2 (Solarbio, Beijing, China), the final concentration of which was 200 μmol/L, the cells in both groups were treated for 24 hours, and then replaced with complete medium to cultivate for 72 hours.

5. Isolation and culture of rat bone marrow-derived MSCs

Bilateral femurs and tibias were harvested under aseptic conditions from SD rats of both control and SONFH groups. The medullary cavity was flushed with low-glucose DMEM (Gibco, USA). Bone marrow tissue was centrifuged at 1000 rpm for 5 minutes to remove suspended adipose tissue. Bone marrow precipitates were then resuspended in complete L-DMEM containing 10% FBS and 1% double-antibody) and cultured at 37 °C / 5% CO_2. After 48 hours, nonadherent cells were removed by replacing the medium. Then, the medium was replaced every 3 days. When the cells reached 80-90% confluence, they were trypsinized, counted, and reseeded as the first passage. Cells from passages 3-6 were used for subsequent experiments.

6. RNA extraction and quantitative real-time RT-PCR

Total RNA was extracted using Trizol reagent (Takara, Japan) according to the manufacturer's instructions. Then, 1 μg of total RNA was reverse-transcribed using PrimeScript RT Master Mix kit (Takara, Japan) for reverse transcription, and used the reverse transcription product for amplification. For miRNA detection, RNA samples were purified and reversed transcribed using the TaqMan microRNA reverse transcription kit (Applied Biosystems, USA). Quantitative PCR was performed using EvaGreeen miRNA qPCR MaterMix (abm, Canada) and SYBR Premix Ex Taq II (TaKaRa, Japan). U6 and β-actin served as the internal control to quantify the relative expression of miRNA and mRNA. We quantified the results by using the $2^{-\Delta\Delta CT}$ method. The specific primers are listed in Supplementary Table 2.

7. Cell transfection, lentivirus infection, and plasmids constructs

The GV272-SIRT1-3 -UTR-WT plasmid, which contains the putative miR-601-binding sites, and the GV272-SIRT1- 3 -UTR-MUT plasmid, whose putative miR-601-binding sites were mutated, were acquired from

Genechem (Shanghai, China). All constructs were confirmed by DNA sequencing. The miR-601 mimics/inhibitor and the negative control (nc) were purchased from GenePharma (Shanghai, China). SIRT1 siRNA was synthesized from Tsingke (Beijing, China). To overexpress SIRT1, pCDNA3.1-FLAG-SIRT1 plasmid and control vector plasmid were obtained from Tsingke (Beijing, China). The relevant sequences were provided in Supplementary Table 2. Lipofectamine 2000 (Invitrogen, Grand Island, NY, USA) was used for transfection following the manufacturer's instructions.

8. Western blotting (WB).

Protein was extracted from the indicated cells using RIPA lysis buffer (Beyotime, Shanghai, China) supplemented with protease inhibitors PMSF (Beyotime, Shanghai, China). The protein concentration was measured using bicinchoninic acid (BCA) protein assay kit (Beyotime, Shanghai, China). Equal amounts of each sample were separated by SDS–polyacrylamide gels and immunoblotted with appropriate antibodies. The primary antibody was used and incubated at 4 °C overnight. The membranes were then incubated with the peroxidase conjugated secondary antibody (Bioworld, 1:10000) for 1 hour at room temperature. The proteins were visualized by an enhanced chemiluminescence assay (Millipore Corporation). The primary antibodies used in WB are listed in Supplementary Table 3. Each experiment was repeated three times,$^{*}P < 0.05$ was considered to be statistically significant.

9. Alizarin red staining (ARS).

After osteogenic induction for 21 days, cells were fixed by 4% paraformaldehyde for 15 minutes, then stained with a 2% alizarin red S solution (Solarbio, Beijing, China) for 10 minutes. These cells were visualized using photography.

10. Oil Red O staining (ORO) and quantification.

After adipogenic induction for 21 days, cells were fixed by 4% paraformaldehyde for 15 minutes, then stained with 0.5% Oil Red O Saturated Solution (Cyagen, USA) for 10 minutes. These cells were visualized under a light microscope. After elution with 100% isopropanol, the absorbance of the eluate at 510 nm was determined by a microplate reader for quantification.

11. SA-β-Gal staining

After the intervention, cells were fixed by SA-β-Gal staining fixative for 15 minutes. An appropriate amount of staining solution (Beyotime, Shanghai, China) was prepared and added to the wells of the plate after washing with PBS. The plate was then placed in a 37 °C incubator (a CO_2 incubator was not used) for 24 hours. Finally, cells were visualized under a light microscope.

12. Hematoxylin and eosin (H&E) staining

The femoral heads were fixed in 4% formaldehyde for 72 hours and decalcified with EDTA decalcification solution for 1 month. After rinsing overnight with running water, the decalcified specimens were

dehydrated with different concentrations of ethanol gradient, hyalinized with xylene and embedded with paraffin. 5 μm thick sections along the coronal planes of femoral heads were made using a paraffin slicer. The sections were stained with hematoxylin-eosin and visualized by microscopy (Olympus).

13. Luciferase reporter assay

Cells cultured in 24-well plates were co-transfected with 1 μg of wide-type or mutated SIRT1 3′ UTR constructs and nc or miR-601 mimics using Lipofectamine 2000 (Invitrogen, Grand Island, NY, USA) according to the manufacturer's instructions. Luciferase activity was measured 48 hours after transfection using the Dual-Glo Luciferase Assay System (Promega, Madison, WI, USA), according to the manufacturer's instructions. Firefly luciferase activity was normalized to Renilla luciferase activity for each sample. Each experiment was repeated three times.

14. Immunohistochemistry (IHC) staining

The sections were dewaxed with xylene and hydrated with gradient ethanol. Then the slides were incubated with hydrogen peroxide to block endogenous peroxidase activity, and the nonspecific binding sites were blocked with goat serum. Then, an appropriate volume of primary antibody was added and placed at 4 °C overnight. On the second day, the samples were incubated with the secondary antibody and the tertiary antibody at room temperature for 30 minutes, stained with diaminobenzidine, and counterstained with hematoxylin. Then, the immunohistochemically stained images were taken under an upright microscope.

15. Statistical analysis

Data analysis was performed using GraphPad Prism 8 software and SPSS 20.0 statistical software. Data are presented as the mean ± standard deviation (SD) of at least three independent experiments. Student's t-test and one-way analysis of variance (ANOVA) followed by Dunnett's post hoc test were used to evaluate the significance of two groups and multiple groups, respectively. $*P < 0.05$ was considered to be statistically significant.

16. Study approval

All experimental procedures involving animals met the relevant guidelines for the humane care of laboratory animals and were approved by the First Affiliated Hospital of Chongqing Medical University and the Ethical Committee of Chongqing Medical University. For human studies, written informed consent was obtained from each donor with the permission of the Institutional Review Board of the First Affiliated Hospital of Chongqing Medical University and approval from the First Affiliated Hospital of Chongqing Medical University and the Ethical Committee of Chongqing Medical University.

Results

1. SONFH accelerated the senescence of BMSCs

To figure out whether BMSCs senescence is affected in SONFH, a rat model of steroid-induced ONFH was established. Empty osteocytic lacunae and trabecular bone and marrow damage were observed in the SONFH group (Fig. 1A). Subsequently, rat BMSCs (rBMSCs) from both the SONFH and control groups were isolated and cultured. Figure 1B shows that the proportion of SA-β-Gal positive rBMSCs in the SONFH rat model was significantly higher than in the control group, indicating that the SONFH group contained more senescent cells. Meanwhile, the mRNA and protein expressions of p16, p21, and p53 in rBMSCs of the SONFH rat model increased significantly (Fig. 1C-D). HBMSCs treated with dexamethasone (10^{-5} M) were used as an SONFH cell model *in vitro*, and SA-β-Gal positive cells in the Dexamethasone group was increased sharply (Fig. 1E). The mRNA and protein expressions of p16, p21, and p53 in the Dexamethasone group were elevated as well (Fig. 1F-G).

2. Senescence inhibited osteogenic differentiation and promoted adipogenic differentiation of BMSCs

To confirm the effect of aging on the adipogenic and osteogenic differentiation of BMSCs, H_2O_2 was used to induce the senescence and degeneration of hBMSCs. It can be seen from Figure 2A that the proportion of SA-β-Gal positive cells in the H_2O_2 group was significantly higher than that in the vehicle group, indicating that there were more senescent cells in the H_2O_2 group. The mRNA expressions of p16, p21, and p53 in the H_2O_2 group increased (Fig. 2B). In addition, the expressions of osteogenic genes (ALP, RUNX2, and OPN) were obviously down-regulated in the H_2O_2 group (Fig. 2C-D), while the expressions of adipogenic genes (PPARγ, C/EBP , and FABP4) were considerably up-regulated (Fig. 2E-F).

3. The expression of SIRT1 is decreased in SONFH

We further explored the mechanism by which GCs induced BMSCs senescence. Silencing SIRT1 not only up-regulated the expression of aging markers but also increased the percentage of SA-β-Gal positive cells (Supplementary Fig. 1A-C). The SIRT1 protein level was reduced in rBMSCs from the SONFH group, while its mRNA level remained unchanged (Fig. 3A-B). *In vitro* studies confirmed the above findings as well (Fig. 3C-D). The effect of SIRT1 on the differentiation of hBMSCs was assessed. Silencing SIRT1 in hBMSCs down-regulated the expression levels of osteogenic genes and up-regulated the expression levels of adipogenic genes, while SIRT1 over-expression exerted the opposite effect (Supplementary Fig. 1D-F).

To make clear the inconsistency between SIRT1 mRNA and protein expression, we tested whether miRNA was involved. The upstream effectors of SIRT1 were identified using the bioinformatics prediction websites miRDB (Target score greater than 90), Targetscan (Context++score percentage greater than 95), and mirDIP (Score class very high) (Fig. 3E, Supplementary Tables. 4-6). A total of 11 miRNAs were found in all three databases, including let-7c-3p, miR-154-3p, miR-487a-3p, miR-211-5p, miR-204-5p, miR-9-5p, miR-601, miR-22-3p, miR-543, miR-6715b-3p, and miR-4670-3p. The expressions of all these 11 miRNAs were examined. As shown in Figure 3F, a significant up-regulation of miR-601 in hBMSCs treated with dexamethasone was noted. The same trend was also observed in the femoral head bone tissues of SONFH patients (Fig. 3G).

4. MiR-601 regulated the adipogenic and osteogenic differentiation of BMSCs

To investigate the role of miR-601 in the adipo-osteogenic differentiation of BMSCs, miR-601 mimics, mimics-nc, miR-601 inhibitor, and inhibitor-nc were transfected into hBMSCs (Fig. 4A). The mRNA and protein levels of osteogenic genes were lowered, while the expression levels of adipogenic genes were significantly elevated (Fig. 4B-G). In addition, Alizarin red S (ARS) staining and oil red O (ORO) staining were performed (Fig. 4H-I), and the cells transfected with miR-601 mimics showed fewer calcium nodules and more small red droplets of oil in the cells. The contrary results were found in the cells transfected with the miR-601 inhibitor.

5. SIRT1 is the direct downstream targets of miR-601.

To further evaluate whether miR-601 directly interacted with SIRT1, the mRNA and protein levels of SIRT1 were examined. Over-expression of miR-601 inhibited SIRT1 expression, whereas silencing miR-601 had the opposite effect (Fig. 5A-B). In addition, the miR-601-binding site was predicted using web-based software, TargetScan. The “CUAGACCA” sequence in the 3' UTR of SIRT1 mRNA was considered to be a putative binding site for miR-601 (Fig. 5C). Moreover, the dual-luciferase UTR vectors carrying the wild-type 3 UTR of SIRT1 (SIRT1 3 UTR WT) and the mutant 3 UTR of SIRT1 (SIRT1 3 UTR MUT) were constructed for luciferase reporter assays. HEK293T cells were transfected with the indicated dual-luciferase vectors together with the control or with miR-601 mimics. As shown in Figure 5D, miR-601 mimics significantly decreased the luciferase activity driven by SIRT1 3 UTR WT. In contrast, miR-601 mimics had no significant effect on the luciferase activity of SIRT1 3 UTR MUT vector. To confirm whether miR-601 regulated adipo-osteogenic differentiation through SIRT1, SIRT1 expression was silenced in hBMSCs. And silencing SIRT1 reversed the regulatory effect of miR-601 on adipo-osteogenic differentiation of hBMSCs (Fig. 5E-F).

6. MiR-601 disturbed the balance of adipo-osteogenic differentiation by accelerating BMSCs senescence

To test whether miR-601 regulated adipo-osteogenic differentiation by accelerating BMSCs senescence, miR-601 was either silenced or over-expressed in hBMSCs. Over-expression of miR-601 in hBMSCs resulted in enhanced senescence, as shown by increased β-galactosidase staining (Fig. 6A) and the up-regulated expression of aging-related genes (i.e., p16, p21, and p53) (Fig. 6B). In contrast, miR-601 silencing decreased β-galactosidase staining and the expressions of aging-related genes (Fig. 6C-D). Furthermore, we demonstrated that SIRT1 silencing in hBMSCs could attenuate senescence (Fig. 6E-F). The induction of hBMSCs senescence was shown to be able to reverse the effect of miR-601 on osteogenic and adipogenic differentiation (Fig. 6G-H). Additionally, the induction of hBMSCs senescence reversed the effect of SIRT1 over-expression as well (Supplementary Fig. 2A-B).

Furthermore, metformin, which is a well-known anti-aging drug [16], was used in the present study. As shown in Supplementary Figure 2C, metformin treatment (5 μM) significantly reduced the expression level of aging-related genes. And metformin treatment could rescue the disordered osteogenic and adipogenic differentiation caused by miR-601 over-expression (Fig. 6I-J).

7. Metformin prevented the progression of SONFH *in vivo*

A rat model of SONFH was established to further validate the therapeutic value of anti-aging treatment *in vivo*. Compared with the SONFH group, metformin treatment reduced the extent of subchondral bone destruction (Fig. 7A), increased the bone volume fraction (BV/TV), and decreased trabecular thickness (Tb.Th), trabecular number (Tb.N), and trabecular separation (Tb. Sp) significantly (Fig. 7B). Less damage to trabecular bone and marrow and fewer empty osteocytic lacunae were shown in the femoral heads of the metformin treatment group (Fig. 7C). IHC staining showed that the expressions of aging-related genes were much lower in the metformin treatment group, while the expression of SIRT1 was significantly increased (Fig. 7D). Meanwhile, miR-601 was silenced in SONFH rats through antagomir. The change trend after miR-601 silencing was the same as that in the metformin treatment group (Fig.7A-7D).

Discussion

Discussion

SONFH is one of the most common complications of GCs use in clinical therapy [1]. The imbalance between osteogenic and adipogenic differentiation of BMSCs is not only a key pathological feature of SONFH, but it also plays a role in its pathogenesis [4]. In this study, we found that in SONFH, GCs accelerated the aging of BMSCs through the miR-601/SIRT1 signaling axis, resulting in disturbed osteogenesis and adipogenesis of BMSCs and accelerated SONFH progression. *In vivo* studies showed that the anti-aging drug metformin or silencing miR-601 maintained the expression level of SIRT1 and prevented SONFH progress in the rat model.

SIRT1, a well-known anti-aging molecule, plays an important role in various aging-related pathological processes, such as inflammation and oxidative stress [14, 17, 18]. And studies have shown that the activation of SIRT1 can promote the osteogenic differentiation of BMSCs and repress the adipogenic differentiation [11]. However, whether SIRT1-mediated BMSCs senescence plays a role in the process of SONFH is still unclear. The present study showed that SIRT1 protein level was significantly decreased in both the SONFH rat model and BMSCs treated with dexamethasone *in vitro*. Down-regulation of SIRT1 has been shown to hasten the aging process and disease progression [19, 20]. Silencing SIRT1 in BMSCs contributed to the aging phenotype, consistent with many other cell types [21]. This study further explored the cause of the down-regulation of SIRT1 in SONFH. In view of the inconsistent changes in SIRT1 mRNA and protein levels, we speculate that post-transcriptional regulation may be involved, such as miRNAs which could target SIRT1 mRNA. MiRNAs bind perfectly or imperfectly to the 3'-untranslated region (3'UTR) of target mRNAs, leading to post-transcriptional repression or mRNA cleavage and then reducing the corresponding protein products. MiRNAs have been well reported to play a comprehensive role in diverse orthopedic diseases. We found that miR-601, which was significantly up-regulated in SONFH, could target SIRT1, down-regulate its expression, and promote the senescence of BMSCs. Although the mechanism by which miR-601 targets SIRT1 has been demonstrated in hepatocellular carcinoma [22],

this study is the first to present a new mechanism by which miR-601 stimulates the progression of SONFH by targeting SIRT1.

However, the specific mechanism by which SIRT1 regulates BMSCs senescence still remains unclear. Interestingly, oxidative stress is thought to be a major contributor to cell senescence [23], as well as an important pathophysiological alteration of SONFH [24]. Dysfunction of the mitochondrial aerobic respiratory chain results in excessive production of active oxygen due to hypoxia in the necrotic area of the femoral head [25]. After femoral head necrosis, a large number of inflammatory cells infiltrated, and these inflammatory cells also produced excessive reactive oxygen species in BMSCs [26]. And SIRT1 can mediate cell aging by participating in the process of oxidative stress [27]. The relationship between oxidative stress and cellular senescence in SONFH deserves further investigation.

Cellular senescence is a stable form of cell-cycle arrest induced by telomere shortening or cellular stress [28]. Cellular senescence is not only involved in the progression of degenerative diseases, such as osteoporosis and intervertebral disc degeneration [29, 30], but also diverse non-degenerative diseases, such as osteosarcoma, osteomyelitis, and ankylosing spondylitis [31, 32]. GCs have been reported to induce senescence in multiple cell lines. Sui et al. showed that GCs could induce BMSCs aging in a rat model of GCs-induced osteoporosis [33]. This study verified the effect of GCs on the aging of BMSCs in a SONFH rat model and BMSCs treated with dexamethasone *in vitro*. In physiological conditions, the adipogenic and osteogenic differentiations of BMSCs are in a dynamic balance. While in various pathophysiological processes, such as aging, obesity, and osteoporosis, the balance is disturbed [8]. Aging could promote adipogenesis and inhibit osteogenesis through activating reactive oxygen species-induced oxidative damage, regulating the expression of osteogenic and adipogenic genes, and inducing cell cycle arrest [8, 10, 11]. However, whether cellular senescence has a role in SONFH remains unclear. This study showed that BMSCs aging could lead to decreased osteogenic differentiation and increased adipogenic differentiation. Moreover, the anti-aging drug metformin was revealed to prevent SONFH progress in a rat model by maintaining the expression level of SIRT1, suggesting the anti-aging therapy of BMSCs to be a promising treatment for SONFH. Anti-aging is a very promising but challenging field. Metformin, which has been a widely prescribed drug in type 2 diabetes treatment over the past century [34], has positive preventive and therapeutic effects on aging-related diseases [35]. However, there is evidence that long-term use of metformin may lead to vitamin B12 deficiency, lactic acid accumulation, and gastrointestinal irritation [36, 37]. Considering that many proteins could be regulated by metformin treatment, uncertainty remains as to whether these proteins display beneficial or potentially harmful off-target effects. Therefore, in follow-up studies, we will further clarify the therapeutic value, clinical safety, and detailed molecular mechanisms of metformin in SONFH treatment.

Moreover, previous studies have found that bone is regulated by osteoblasts and osteoclasts, and cell types such as osteocytes, bone lining cells, osteomacs, and vascular endothelial cells in the basic multicellular unit [38]. In addition to BMSCs, does knockdown of miR-601 and metformin also affect these cells? This point is also worthy of our further exploration.

Conclusion

In conclusion, this study revealed for the first time that cellular senescence was involved in the progression of SONFH and elucidated the molecular mechanism that caused BMSCs senescence in SONFH. In addition, it was preliminarily verified that metformin prevented the progression of SONFH by inhibiting BMSC senescence. Therefore, BMSCs senescence holds promise as a new therapeutic target for SONFH. Further research will focus on the mechanism through which SIRT1 mediates BMSCs senescence and confirming the clinical value of anti-aging therapy in the treatment of SONFH.

Abbreviations

ALP: Alkaline phosphatase

ARS: Alizarin red staining

BMSCs: Bone marrow mesenchymal stem cells

BV/TV: Bone volume per tissue volume

C/EBP ：CCAAT-enhancer-binding proteins

FABP4: Fatty acid-binding protein 4

FNF: Femoral neck fracture

GCs: Glucocorticoids

H&E: Hematoxylin and eosin staining

IHC: Immunohistochemistry

LPS: Lipopolysaccharide

MPS: Methylprednisolone

OPN: Osteopontin

ORO: Oil Red O staining

PPARγ: Peroxisome proliferators-activated receptors γ

RUNX2: Runt-related transcription factor 2

SIRT1: Sirtuin1

SONFH: Steroid-induced osteonecrosis of the femoral head

Tb.N: Trabecular number

Tb.Sp: Trabecular separation

Tb.Th: Trabecular thickness

Declarations

Ethics approval and consent to participate.

(1) Title of the approved project: The role and molecular mechanism of miRNA-601 in steroid-induced necrosis of the femoral head; (2) Name of the institutional approval committee or unit: The First Affiliated Hospital of Chongqing Medical University and the Ethical Committee of Chongqing Medical University; (3) Approval number: 2022-005; (4) Date of approval: March 23, 2022.

Consent for publication

Not applicable.

Availability of data and materials

The data that support the fndings of this study are available from the Corresponding authors upon reasonable request.

Competing interests

The authors declare that they have no competing interests.

Funding

The study was supported by the Natural Science Foundation of China (No. 32271179, 8210090704); Chongqing Technology Innovation and Application Development Project (CQYC202010); the Natural Science Foundation of Chongqing Science and Technology Commission (No. cstc2020jcyj-msxmX0179); the Science Foundation for Top-notch Young Scholars of the First Affiliated Hospital of Chongqing Medical University (No. BJRC2021-02); the Science and Technology Research Project of Chongqing Sports Bureau (No. A202206, A202013); and the Science and Technology Research Project of Chongqing Education Commission (No. KJQN202200404). All the funding body played no role in the design of the study and collection, analysis, and interpretation of data and in writing the manuscript.

Author contributions:

J.Z, C.L. and B.T. participated in the design of the study and carried out experiments. B.T., Y.C., M.S., H.Z., and D.X. conceived the experiments. B.T, P.Z, W.Y, X.H. and T.C. analyzed the data. B.T., C.L. and J.Z. wrote the manuscript. All authors were involved in writing the paper and had final approval of the submitted and published versions.

Acknowledgements

Not applicable.

References

1. Zaidi M, Sun L, Robinson LJ, Tourkova IL, Liu L, Wang Y, et al. ACTH protects against glucocorticoid-induced osteonecrosis of bone. Proc Natl Acad Sci U S A. 2010;107(19):8782-7.
2. Zhao D, Xie H, Xu Y, Wang Y, Yu A, Liu Y, et al. Management of osteonecrosis of the femoral head with pedicled iliac bone flap transfer: A multicenter study of 2190 patients. Microsurgery. 2017;37(8):896-901.
3. Zhao D, Zhang F, Wang B, Liu B, Li L, Kim SY, et al. Guidelines for clinical diagnosis and treatment of osteonecrosis of the femoral head in adults (2019 version). J Orthop Translat. 2020;21:100-10.
4. Han L, Wang B, Wang R, Gong S, Chen G, Xu W. The shift in the balance between osteoblastogenesis and adipogenesis of mesenchymal stem cells mediated by glucocorticoid receptor. Stem Cell Res Ther. 2019;10(1):377.
5. Zhu W, Guo M, Yang W, Tang M, Chen T, Gan D, et al. CD41-deficient exosomes from non-traumatic femoral head necrosis tissues impair osteogenic differentiation and migration of mesenchymal stem cells. Cell Death Dis. 2020;11(4):293.
6. Tan G, Kang PD, Pei FX. Glucocorticoids affect the metabolism of bone marrow stromal cells and lead to osteonecrosis of the femoral head: a review. Chin Med J (Engl). 2012;125(1):134-9.
7. Muñoz-Espín D, Serrano M. Cellular senescence: from physiology to pathology. Nat Rev Mol Cell Biol. 2014;15(7):482-96.
8. Chen Q, Shou P, Zheng C, Jiang M, Cao G, Yang Q, et al. Fate decision of mesenchymal stem cells: adipocytes or osteoblasts? Cell Death Differ. 2016;23(7):1128-39.
9. Hernandez-Segura A, Nehme J, Demaria M. Hallmarks of Cellular Senescence. Trends Cell Biol. 2018;28(6):436-53.
10. Moerman EJ, Teng K, Lipschitz DA, Lecka-Czernik B. Aging activates adipogenic and suppresses osteogenic programs in mesenchymal marrow stroma/stem cells: the role of PPAR-gamma2 transcription factor and TGF-beta/BMP signaling pathways. Aging Cell. 2004;3(6):379-89.
11. Chen H, Liu X, Chen H, Cao J, Zhang L, Hu X, et al. Role of SIRT1 and AMPK in mesenchymal stem cells differentiation. Ageing Res Rev. 2014;13:55-64.
12. Chen C, Zhou M, Ge Y, Wang X. SIRT1 and aging related signaling pathways. Mech Ageing Dev. 2020;187:111215.
13. Sasaki T, Maier B, Bartke A, Scrable H. Progressive loss of SIRT1 with cell cycle withdrawal. Aging Cell. 2006;5(5):413-22.
14. Xu C, Wang L, Fozouni P, Evjen G, Chandra V, Jiang J, et al. SIRT1 is downregulated by autophagy in senescence and ageing. Nat Cell Biol. 2020;22(10):1170-9.

15. McBurney MW, Yang X, Jardine K, Hixon M, Boekelheide K, Webb JR, et al. The mammalian SIR2alpha protein has a role in embryogenesis and gametogenesis. Mol Cell Biol. 2003;23(1):38-54.
16. Kulkarni AS, Gubbi S, Barzilai N. Benefits of Metformin in Attenuating the Hallmarks of Aging. Cell Metab. 2020;32(1):15-30.
17. Ramis MR, Esteban S, Miralles A, Tan DX, Reiter RJ. Caloric restriction, resveratrol and melatonin: Role of SIRT1 and implications for aging and related-diseases. Mech Ageing Dev. 2015;146-148:28-41.
18. Finkel T, Deng CX, Mostoslavsky R. Recent progress in the biology and physiology of sirtuins. Nature. 2009;460(7255):587-91.
19. Barnes PJ, Baker J, Donnelly LE. Cellular Senescence as a Mechanism and Target in Chronic Lung Diseases. Am J Respir Crit Care Med. 2019;200(5):556-64.
20. Ong ALC, Ramasamy TS. Role of Sirtuin1-p53 regulatory axis in aging, cancer and cellular reprogramming. Ageing Res Rev. 2018;43:64-80.
21. Duan JL, Ruan B, Song P, Fang ZQ, Yue ZS, Liu JJ, et al. Shear stress-induced cellular senescence blunts liver regeneration through Notch-sirtuin 1-P21/P16 axis. Hepatology. 2022;75(3):584-99.
22. Song W, Wenhui Z, Ruiqiang Y, Hu X, Shi T, Wang M, et al. Long noncoding RNA PP7080 promotes hepatocellular carcinoma development by sponging mir-601 and targeting SIRT1. Bioengineered. 2021;12(1):1599-610.
23. Wei W, Ji S. Cellular senescence: Molecular mechanisms and pathogenicity. J Cell Physiol. 2018;233(12):9121-35.
24. Chen K, Liu Y, He J, Pavlos N, Wang C, Kenny J, et al. Steroid-induced osteonecrosis of the femoral head reveals enhanced reactive oxygen species and hyperactive osteoclasts. Int J Biol Sci. 2020;16(11):1888-900.
25. McGarry T, Biniecka M, Veale DJ, Fearon U. Hypoxia, oxidative stress and inflammation. Free Radic Biol Med. 2018;125:15-24.
26. Sung YJ, Kao TY, Kuo CL, Fan CC, Cheng AN, Fang WC, et al. Mitochondrial Lon sequesters and stabilizes p53 in the matrix to restrain apoptosis under oxidative stress via its chaperone activity. Cell Death Dis. 2018;9(6):697.
27. Hwang JW, Yao H, Caito S, Sundar IK, Rahman I. Redox regulation of SIRT1 in inflammation and cellular senescence. Free Radic Biol Med. 2013;61:95-110.
28. Campisi J, d'Adda di Fagagna F. Cellular senescence: when bad things happen to good cells. Nat Rev Mol Cell Biol. 2007;8(9):729-40.
29. Pignolo RJ, Law SF, Chandra A. Bone Aging, Cellular Senescence, and Osteoporosis. JBMR Plus. 2021;5(4):e10488.
30. Du J, Xu M, Kong F, Zhu P, Mao Y, Liu Y, et al. CB2R Attenuates Intervertebral Disc Degeneration by Delaying Nucleus Pulposus Cell Senescence through AMPK/GSK3β Pathway. Aging Dis. 2022;13(2):552-67.

31. Hsu YK, Chen HY, Wu CC, Huang YC, Hsieh CP, Su PF, et al. Butein induces cellular senescence through reactive oxygen species-mediated p53 activation in osteosarcoma U-2 OS cells. Environ Toxicol. 2021;36(5):773-81.
32. González-Osuna L, Sierra-Cristancho A, Rojas C, Cafferata EA, Melgar-Rodríguez S, Cárdenas AM, et al. Premature Senescence of T-cells Favors Bone Loss During Osteolytic Diseases. A New Concern in the Osteoimmunology Arena. Aging Dis. 2021;12(5):1150-61.
33. Sui B, Hu C, Liao L, Chen Y, Zhang X, Fu X, et al. Mesenchymal progenitors in osteopenias of diverse pathologies: differential characteristics in the common shift from osteoblastogenesis to adipogenesis. Sci Rep. 2016;6:30186.
34. Pryor R, Cabreiro F. Repurposing metformin: an old drug with new tricks in its binding pockets. Biochem J. 2015;471(3):307-22.
35. Ou Z, Kong X, Sun X, He X, Zhang L, Gong Z, et al. Metformin treatment prevents amyloid plaque deposition and memory impairment in APP/PS1 mice. Brain Behav Immun. 2018;69:351-63.
36. Langan RC, Goodbred AJ. Vitamin B12 Deficiency: Recognition and Management. Am Fam Physician. 2017;96(6):384-9.
37. McCreight LJ, Stage TB, Connelly P, Lonergan M, Nielsen F, Prehn C, et al. Pharmacokinetics of metformin in patients with gastrointestinal intolerance. Diabetes Obes Metab. 2018;20(7):1593-601.
38. Kular J, Tickner J, Chim SM, Xu J. An overview of the regulation of bone remodelling at the cellular level. Clin Biochem. 2012;45(12):863-73.

Figures

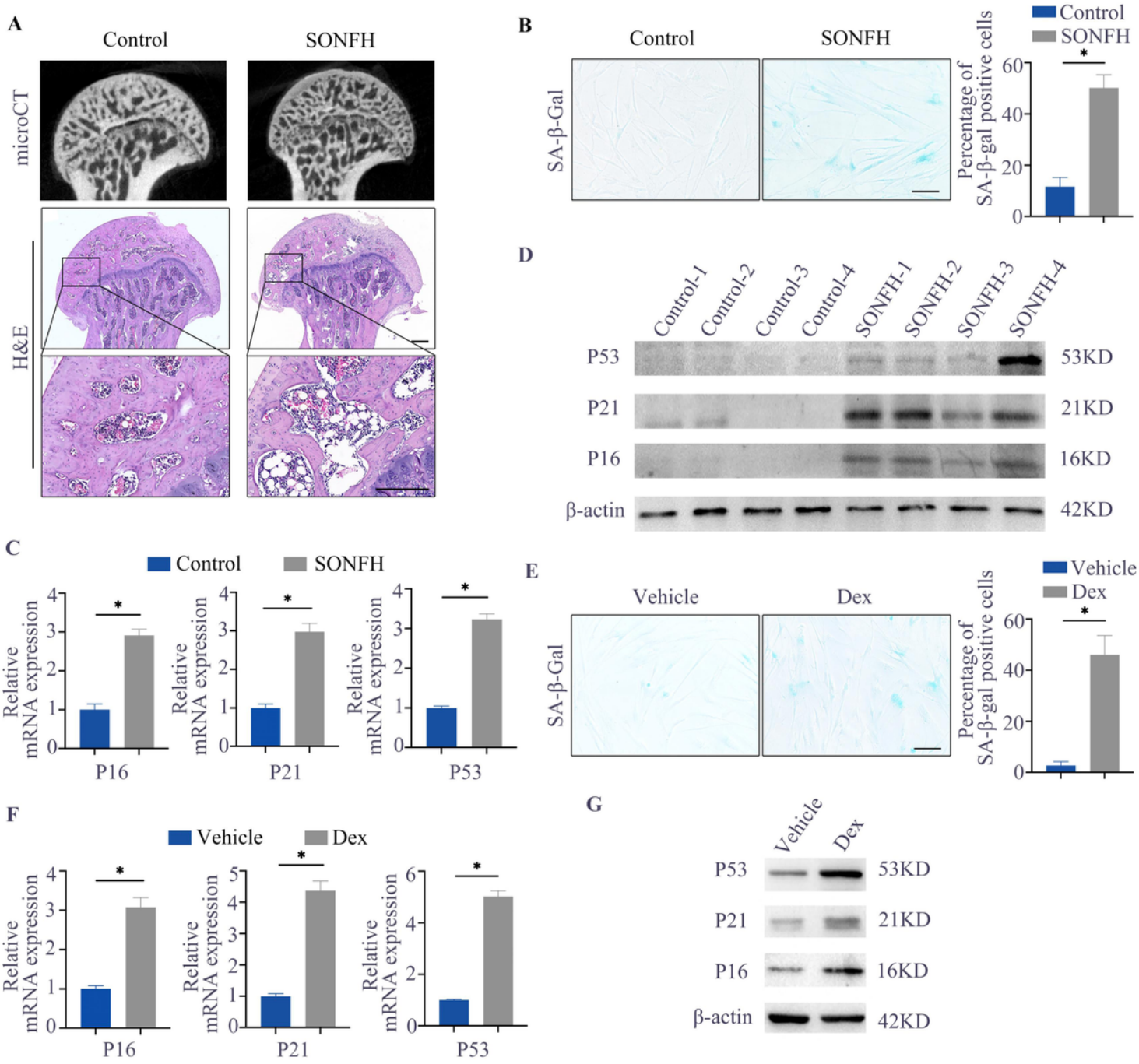

Figure 1

SONFH accelerated the senescence of BMSCs.

(A) A rat SONFH model was constructed. Representative μCT-reconstructed images and H&E staining images of rat femoral heads were presented.

(B-D) RBMSCs were isolated from rat model. SA-β-Gal staining and quantitative analysis were conducted (B). The mRNA and protein expressions of p16, p21, p53 were tested by RT-qPCR (C) and Western blotting (D).

(E-G) HBMSCs were treated with Dexamethasone (10^{-5}M) or vehicle for 48 hours, and the proportion of SA-β-Gal positive cells was detected by SA-β-Gal staining (E). The expression levels of P16, P21, and P53 were detected by RT-qPCR (F) and Western blotting (G).

Scale bars in A, 100 μm; Scale bars in B, 200 μm; Dex, dexamethasone; *$P < 0.05$.

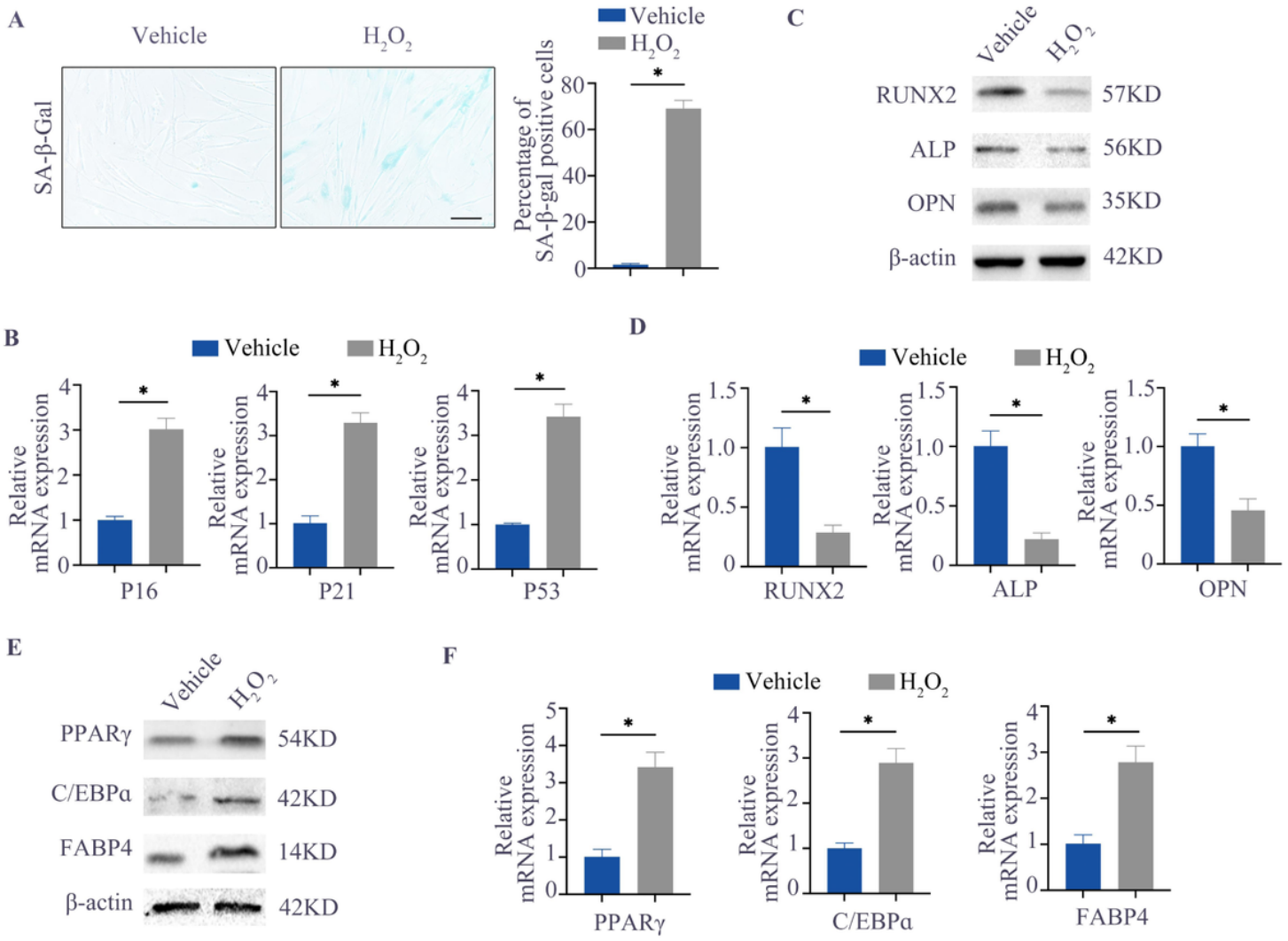

Figure 2

Senescence inhibited osteogenic differentiation and promoted adipogenic differentiation of BMSCs.

(A, B) HBMSCs were treated with H_2O_2 (500 μmol /L) or vehicle for 24 hours. The proportion of SA-β-Gal positive cells was detected by SA-β-Gal staining (A), and the mRNA expressions of p16, p21, and p53 were measured by RT-qPCR (B).

(C, D) The expression levels of osteogenic-related genes were detected by Western blotting (C) and RT-qPCR (D).

(E, F) The expression levels of adipogenic-related genes were detected by Western blotting (E) and RT-qPCR (F).

Scale bars in A, 100 μm; *$P < 0.05$.

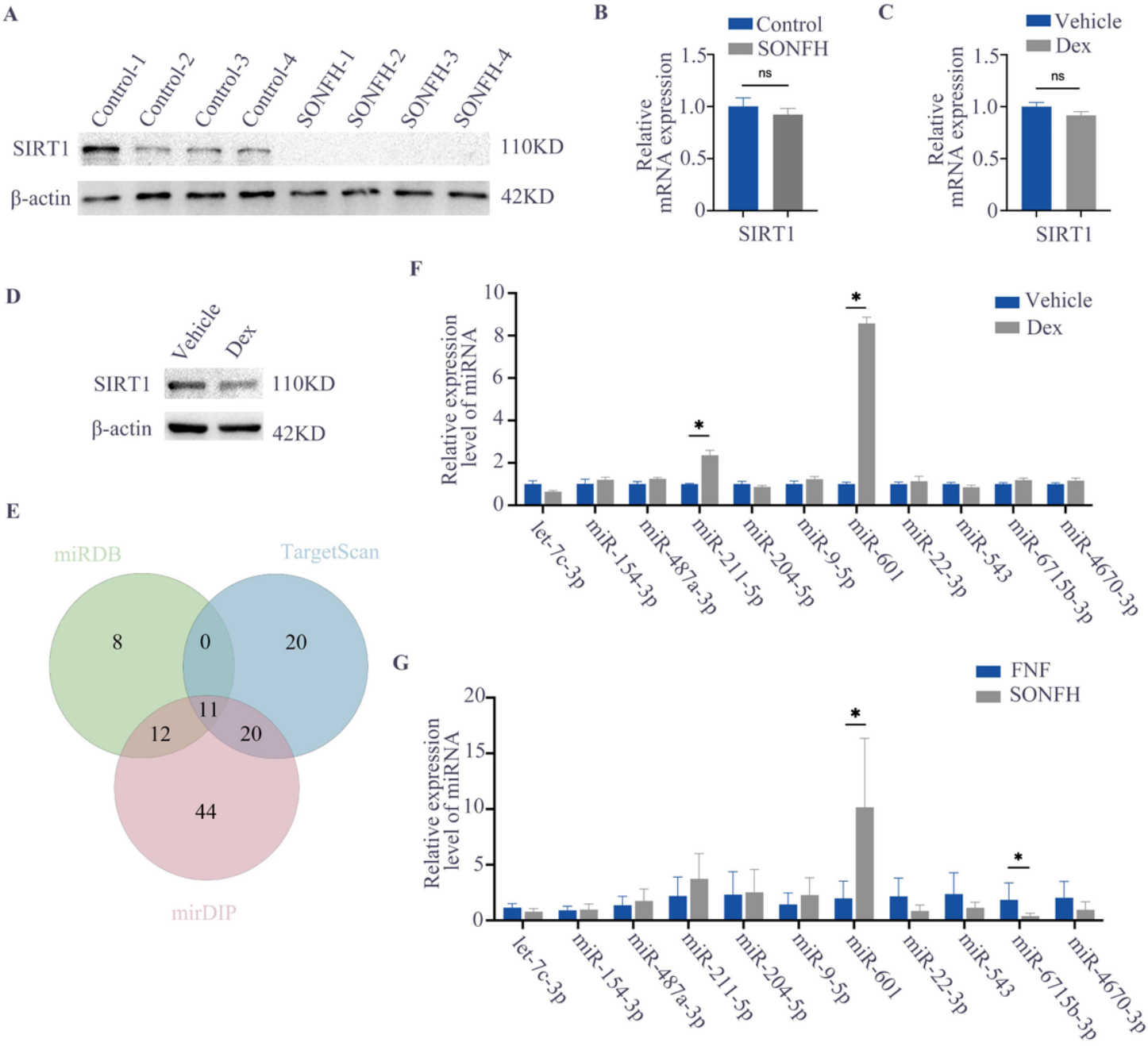

Figure 3

The expression of SIRT1 is decreased in SONFH.

(A, B) SIRT1 expression was detected by Western blotting (A) and RT-qPCR (B) in rBMSCs from control and SONFH groups.

(C, D) HBMSCs were treated with dexamethasone (10^{-5}M) or vehicle for, and SIRT1 expression was detected by RT-qPCR (C) and Western blotting (D).

(E) Venn diagrams represent the common potential target genes of SIRT1 predicted by miRDB (Target score is greater than 90), Targetscan (Context++score percentage is greater than 95), and mirDIP (Score Class is Very High).

(F) RT-qPCR analyses of the eligible miRNAs in hBMSCs treated with Dexamethasone (10^{-5}M) or vehicle.

(G) The expressions of the above eligible miRNAs were detected by RT-qPCR in the bone tissues obtained from the femoral heads of FNF and SONFH patients.

Dex, dexamethasone; ns, no significance; FNF, femoral neck fracture; *$P < 0.05$.

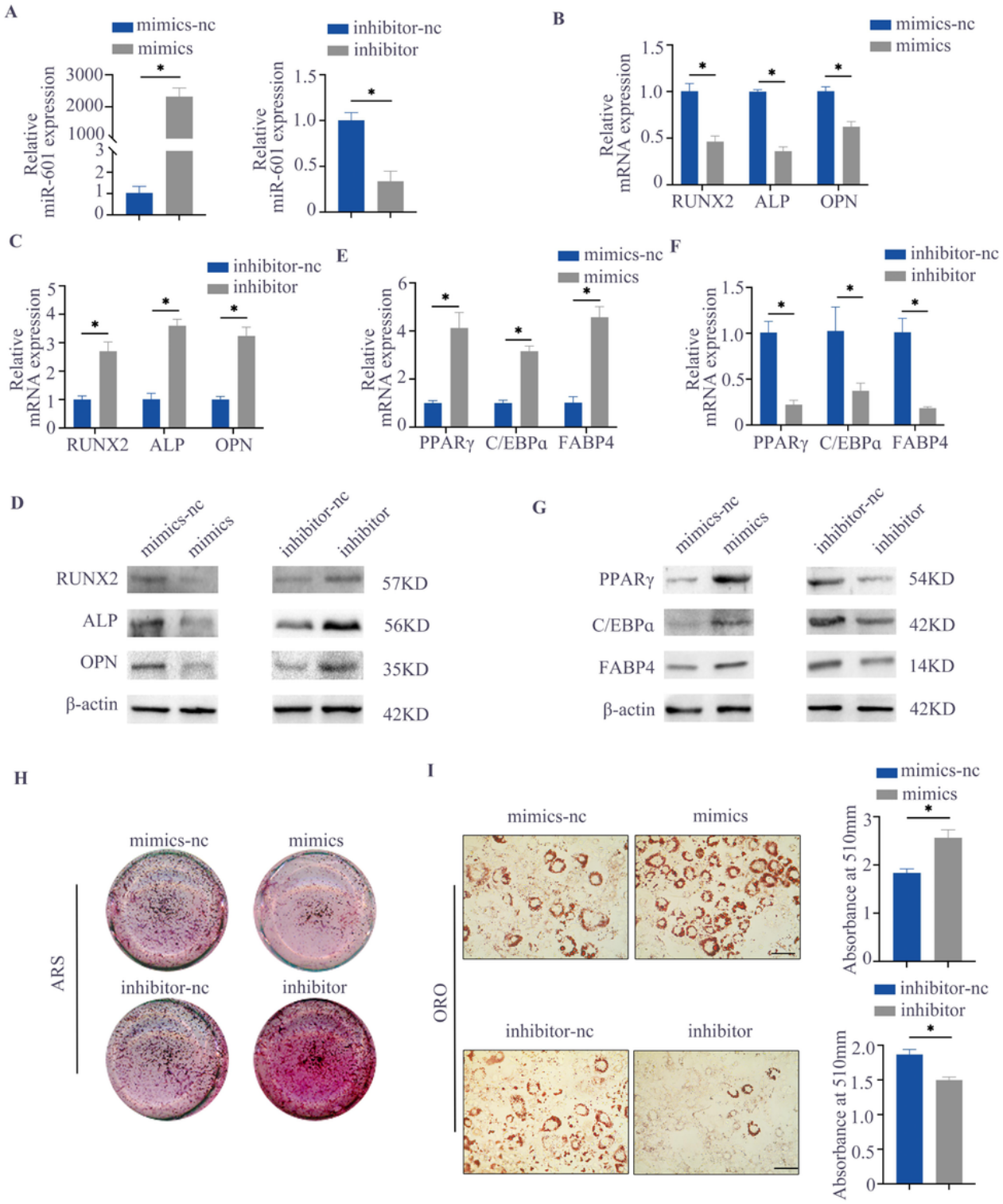

Figure 4

MiR-601 regulated the adipogenic and osteogenic differentiation of BMSCs.

(A)RT-qPCR analyses to assess the expression of miR-601 in hBMSCs after miR-601 mimics, mimics-nc, miR-601 inhibitor, or inhibitor-nc transfection.

(B-D) The expression of osteogenic-related genes was detected by RT-qPCR (B, C) and Western blotting (D).

(E-G) The expression of adipogenic-related genes was detected by RT-qPCR (E, F) and Western blotting (G).

(H) Alizarin red staining of hBMSCs with the indicated constructs after 21 days of culture in osteogenic medium

(I) Oil red staining of BMSCs with the indicated constructs after 21 days of culture in adipogenic medium.

Scale bars in H and G, 100 μm; ARS, alizarin red staining; ORO, Oil red staining; *P< 0.05.

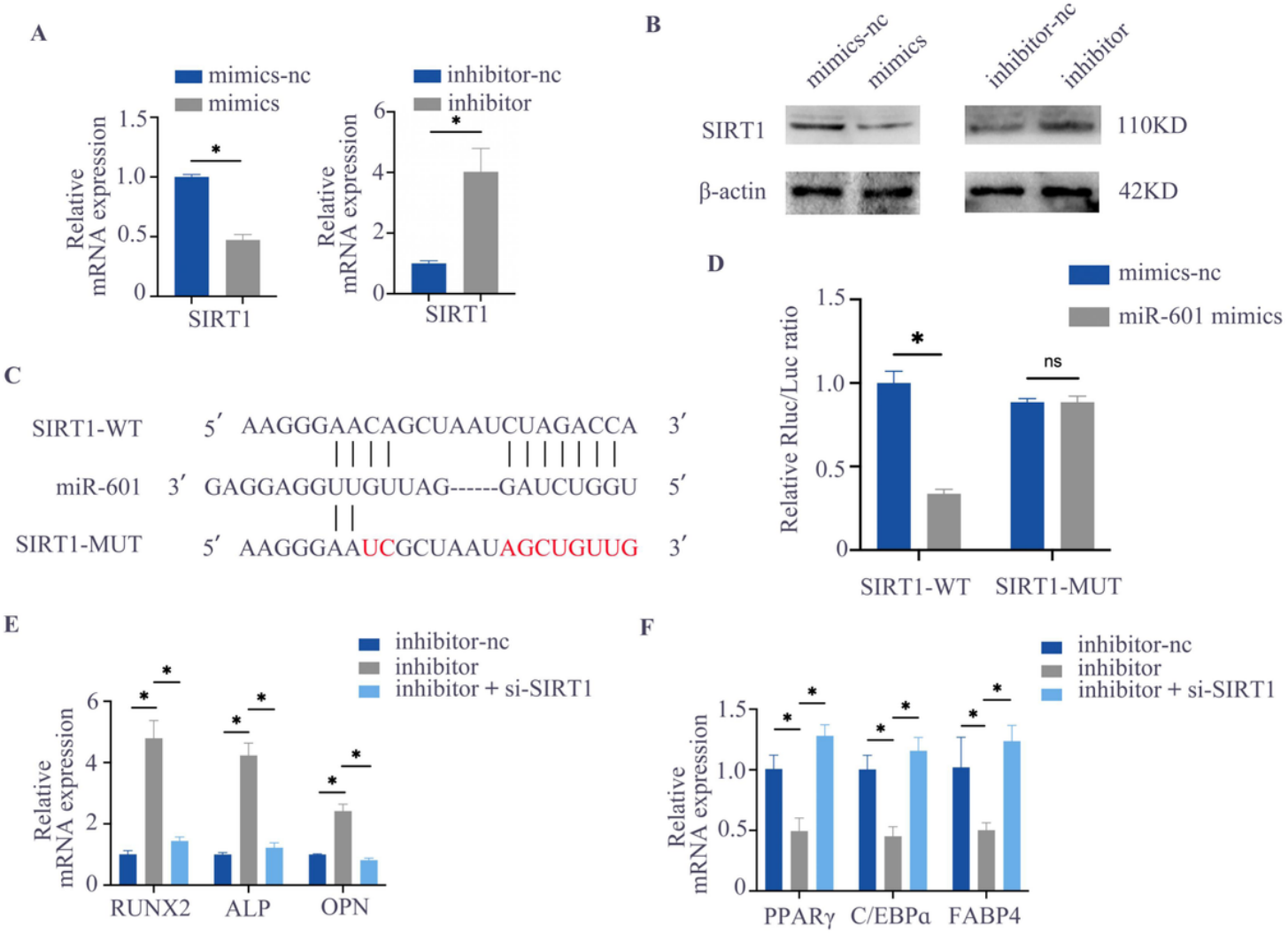

Figure 5

SIRT1 is the direct downstream targets of miR-601.

(A, B) A rat SONFH model was constructed.,and SIRT1 expression was detected by RT-qPCR (A) and Western blotting (B).

(C) The sequence region of miR-601 targeted to SIRT1 was predicted online by Targetscan. The figure shows the binding site and design of the mutation sequence of the site.

(D) Luciferase reporter assays in HEK293T cells 48 hours after co-transfection of the indicated luciferase reporter constructs and miRNAs.

(E, F) Silencing SIRT1 reversed the regulatory effect of miR-601 on the adipo-osteogenic differentiation of hBMSCs

WT, wild type; MUT, mutation; *$P < 0.05$.

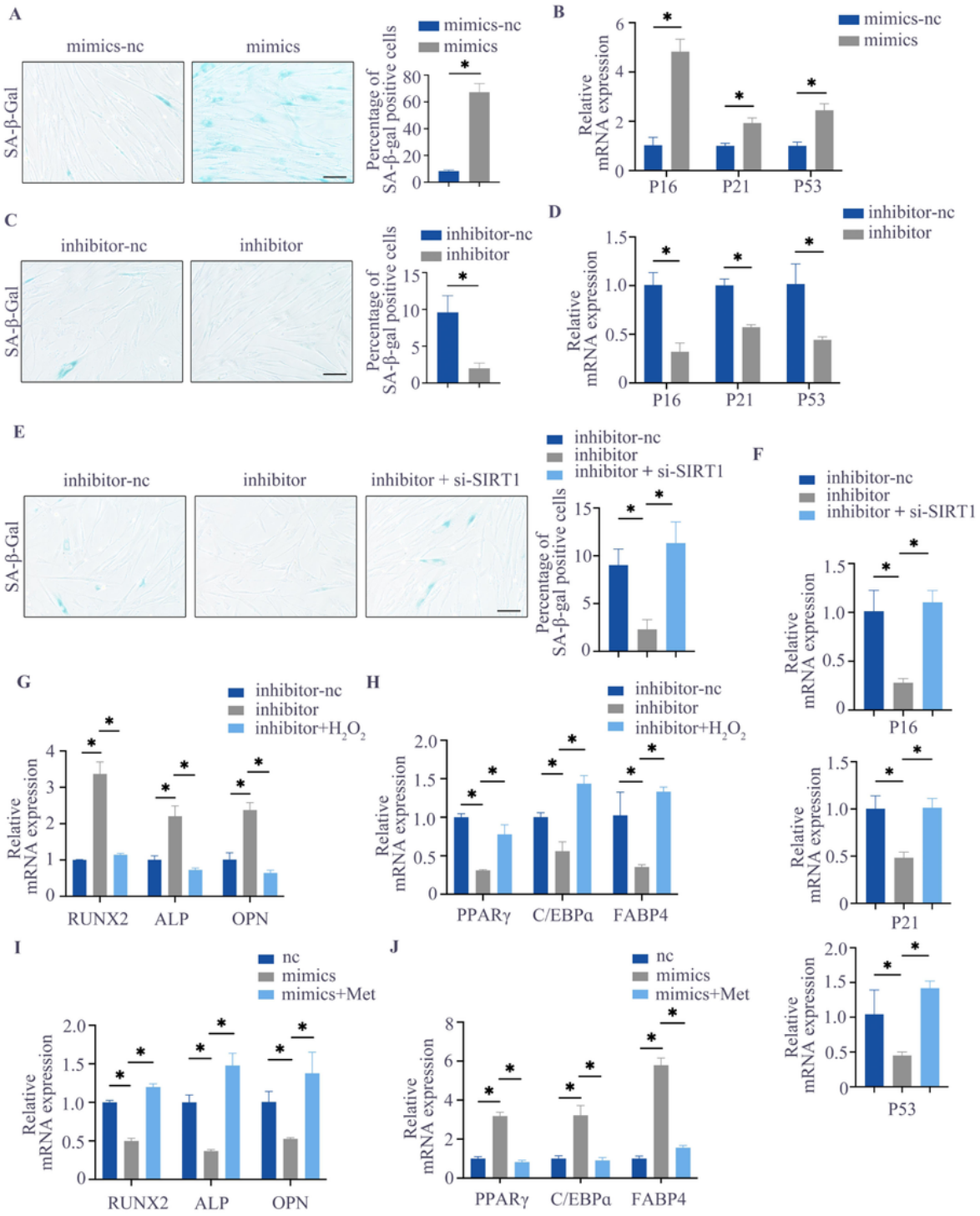

Figure 6

MiR-601 disturbed the balance of adipo-osteogenic differentiation by accelerating BMSCs senescence.

(A-D) HBMSCs were transfected with miR-601 mimics, mimics-nc, miR-601 inhibitor, and inhibitor-nc. SA-β-Gal staining (A, C) and RT-qPCR (B, D) were conducted.

(E, F) Silencing SIRT1 reversed the regulatory effect of miR-601 on the senescence of hBMSCs.

(G-H) HBMSCs were treated with H_2O_2 for 24 hours after miR-601 inhibitor transfection, and the expressions of osteogenic (G) and adipogenic genes (H) were detected by RT-qPCR.

(I-J) HBMSCs were treated with metformin after miR-601 mimics transfection, and the expressions of osteogenic (I) and adipogenic (J) genes were detected by RT-qPCR.

Scale bars in A, B and E, 100 μm; Met, metformin; *$P < 0.05$.

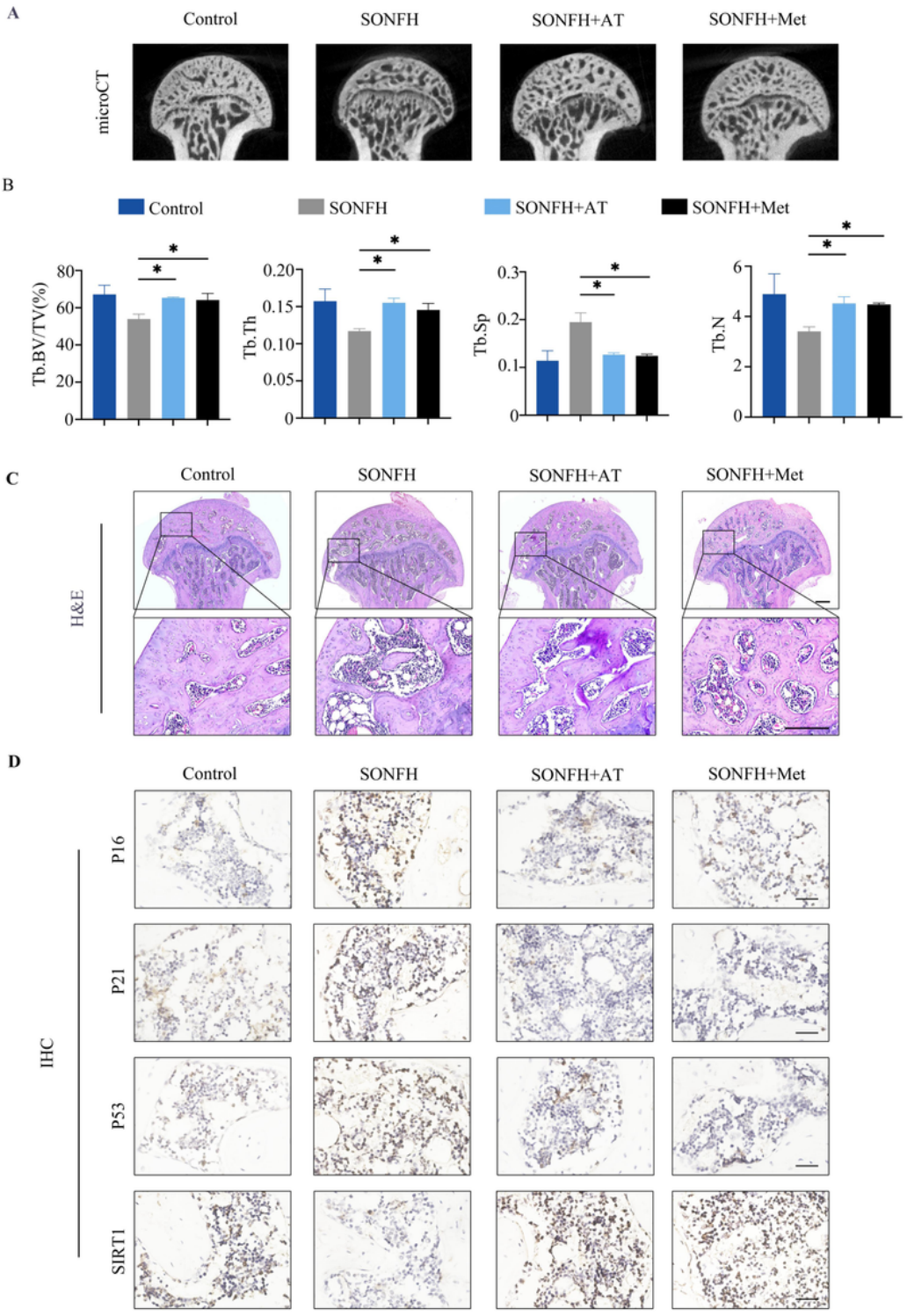

Figure 7

Metformin prevented the progression of SONFH *in vivo*.

(A, B) A rat SONFH model was constructed, and miR-601 antagomir and metformin were used for treatment. Representative μCT-reconstructed images of rat femoral heads (A) and quantification of Tb. BV/TV, Tb. Th, Tb. N, and Tb. Sp (B) were presented.

(C) Representative H&E stainings of rat femoral heads.

(D) IHC staining of P16, P21, P53 and SIRT1 in rat femoral heads.

Scale bars in C, 200 μm; Scale bars in D, 100 μm; Tb. BV/TV, trabecular bone volume fraction; Tb. Th, trabecular thickness; Tb. N, trabecular number; Tb. Sp, trabecular Separation; Met, metformin; ns, no significance; *P < 0.05.

Supplementary Files

This is a list of supplementary files associated with this preprint. Click to download.

- AuthorChecklistscrt.pdf
- SupplementaryMaterials.pdf
- WB.pdf